Damage Diagnosis of Rotors: Application of Hilbert Transform and Multihypothesis Testing

MICHAEL FELDMAN
Faculty of Mechanical Engineering, Technion–Israel Institute of Technology, Haifa 32000, Israel

SUSANNE SEIBOLD
Institut für Techno- und Wirtschaftsmathematik, Erwin-Schrödinger-Straße, D-67663 Kaiserslautern, Germany

(Received 15 January 1997; accepted 15 September 1997)

Abstract: In this paper, a combined approach to damage diagnosis of rotors is proposed. The intention is to employ signal-based as well as model-based procedures for an improved detection of size and location of the damage. In the first step, Hilbert transform signal-processing techniques allow for a computation of the signal envelope and the instantaneous frequency, so that various types of nonlinearities due to damage may be identified and classified based on measured response data. In the second step, a multihypothesis bank of Kalman filters is employed for the detection of the size and location of the damage based on the information of the type of damage provided by the results of the Hilbert transform.

Key Words: Hilbert transform, damage diagnosis, Kalman filtering, nonlinear dynamics

1. INTRODUCTION

Modern machinery is bound to fulfill increasing demands concerning durability as well as safety requirements. To manage these complex tasks, procedures for automated damage detection have to be provided. Current trends are described (e.g., Williams and Davies, 1992). The diagnosis of turbomachinery is of particular relevance to avoid catastrophic damage or injury (Haas, 1977; Muszynska, 1992). Basically, one can distinguish between signal-based approaches, which merely rely on an analysis of the measurements, and model-based approaches, which in addition use an appropriate model of the system under investigation.

Signal-based diagnosis employs our physical understanding of the dynamic system behavior in the presence of a specific damage. For instance, a crack in a rotor shaft influences the rotor vibrations, especially the first, second, and third harmonics. Besides, a shifting of the phase occurs. Therefore, a suitable analysis of the measurement signals yields valuable hints for the detection of a crack. Furthermore, nonlinearities due to the "breathing" (the opening and closing of the crack) are introduced.

Recently, the characterization of the response of nonlinear vibration systems has been approached using the Hilbert transform (HT) in the time domain. The objective was to propose a methodology to identify and classify various types of nonlinearities from measured

Journal of Vibration and Control, **5**: 421-442, 1999

response data (Feldman, 1994a, 1994b). The proposed methodology also concentrated on the HT signal-processing techniques, which allow for the computation of the signal envelope and the instantaneous frequency. It was shown that the system instantaneous dynamic parameters and also the elastic nonsymmetric force characteristics can be estimated (Feldman, 1997). The results showed that the methodology is also well applicable to the diagnosis of damage.

In general, the drawback of the signal-based procedures is that most of the time, the determination of the location and extent of a damage is not possible. This gap can be filled by model-based procedures, in which a numerical relation between the damage and a specific damage parameter is established. The detection is performed by relating algorithmically a model of the system under investigation to the measurements. A suitable analysis of the differences between model and measurements yields the determination of the location and size of the damage. For instance, a bank of Kalman filters may be employed for the detection of the location of a damage such as a crack in a rotor shaft. Furthermore, its depth may be calculated (Seibold and Weinert, 1996).

However, this model-based approach is quite time-consuming and usually not applicable for on-line monitoring. Furthermore, it might sometimes be difficult to distinguish between specific damages such as a crack and an increasing unbalance. Therefore, we propose to combine the two methods for improved detectability of damage at early stages: the HT signal-processing technique will be employed for a characterization of the damage, so that in the second step, a bank of Kalman filters based on a suitable model of the damage can be designed. Then, the location and extent of the damage can be calculated.

This paper is organized according to the following: Section 2 focuses on the HT. First, the theoretical background is explained. Then, a new approach for the application to nonlinear systems is discussed. Section 3 aims at clarifying the procedure with a simulation study. In Section 4, some basic ideas for the modeling of a crack in a rotor shaft are presented, and a finite crack model is described. Section 5 briefly discusses the idea of multihypothesis testing based on a bank of Kalman filters. Finally, in Section 6, the methods presented are applied for the diagnosis of a crack in the shaft of a rotor test rig. Section 7 discusses the results.

2. THEORETICAL BACKGROUND: THE HILBERT TRANSFORM

The considered HT identification methods in the time domain have been developed by one of the authors for only symmetrical nonlinearities (Feldman, 1985, 1994a). As only symmetrical nonlinearities were considered, the nonlinear elastic and damping force characteristic can be expressed in terms of odd polynomials. However, it is also possible to extend the method to analyze vibration systems with nonsymmetrical nonlinearities. The main idea of the method is to take the solution of the nonsymmetrical vibration system in the time domain and split it into two different subsolutions separately for the positive and negative displacement. Then, the separated solutions of the nonsymmetric system are determined by adopting the method developed for the nonlinear vibration system identification (Feldman, 1985, 1994a).

2.1. Nonlinear System Representation

The equation of the free vibration of a nonlinear, nonsymmetrical structure can be written as follows:

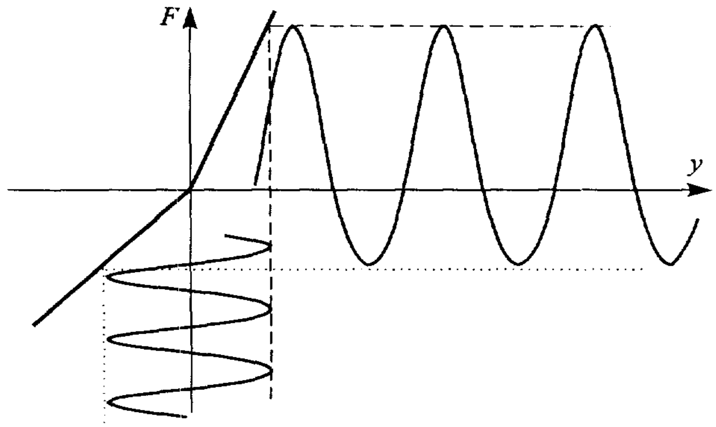

Figure 1. Illustration of the transformation of amplitude of the vibration solution.

$$\ddot{y} + 2h\dot{y} + F(y) = 0,$$

$$F(y) = \begin{cases} F_1(y), & \text{if } y > 0 \\ F_2(y), & \text{if } y \leq 0 \end{cases}, \tag{1}$$

where y is the system solution; h is the damping coefficient; $F(y)$ is the nonlinear, nonsymmetrical spring force; $F_1(y)$ is the nonlinear stiffness characteristic for the positive displacement; and $F_2(y)$ is the nonlinear stiffness characteristic for the negative displacement. The solution of the equation depends mainly on the nonsymmetrical elastic force $F(y)$, which can be expressed in terms of odd and even polynomials of displacement. In the case of positive displacement $y > 0$, the solution is produced by the first line of the nonsymmetrical elastic force characteristic (see Figure 1). Each displacement sign changing from positive to negative, or the reverse, switches the vibration structure, which will include correspondingly the first or the second nonsymmetrical elastic force characteristic. The oscillating force will be transformed into oscillatory motion with corresponding amplitude and frequency features. An illustration of nonsymmetrical amplitude transformation of the solution is shown in Figure 1.

Suppose the solution of the system consists of two independent separate parts: a positive motion, associated only with the positive force characteristic curve, and a negative motion, associated only with the negative force characteristic curve:

$$y(t) = \begin{cases} y_1(t), & \text{if } y > 0 \\ y_2(t), & \text{if } y \leq 0 \end{cases}. \tag{2}$$

The positive motion is only influenced by the positive force, and conversely, the negative motion is dependent on the negative branch. In other words, according to this assumption, each part of the system solution is determined only by its corresponding force characteristic. Each part of the vibration signal could be represented in the analytic signal form $y_{1,2}(t) = A_{1,2}(t)\cos\left[\int \omega_{1,2}(t)\right]$, where $y_i(t)$ is the vibration signal (real valued function), $A_i(t)$ is the envelope (instantaneous amplitude), and $\omega_i(t)$ is the instantaneous frequency. One question that arises immediately from this representation is, How will the combined signal $y(t)$ be separated into its constituent parts $y_1(t)$ and $y_2(t)$? The HT also could play an important role in the signal decomposition and may lead to practical results.

2.2. Bilinear System Vibration Decomposition

First consider the case of a vibrating conservative system with a bilinear force-elastic characteristic $F_{1,2} = \omega_{1,2}^2 y$. According to the assumption of equation (2), the solution of the system is built up from two alternate harmonics. During half of the period, when the displacement is positive, the vibration appears as a harmonic $A_1 \cos \omega_1 t$; during the next half, when the displacement is negative, the vibration continues as another harmonic with the different amplitude and frequency $A_2 \cos \omega_2 t$. As a first approximation, assume that these harmonics have the same frequency and different amplitudes ($A_1 > A_2$). In this case, the signal can be modeled in the time domain as a monocomponent signal $y(t)$ with nonzero mean value M. That is,

$$y(t) = A_m \cos(\omega_m t) + M, \tag{3a}$$

where $A_m = 0.5(A_1 + A_2)$ is the amplitude of the harmonic, and $M = 0.5(A_1 - A_2)$ is the mean value (offset) of the nonsymmetric signal $y(t)$. According to the main properties of the HT (Mitra and Kaiser, 1993), the Hilbert-transformed projection $\tilde{y}(t)$ will not respond to the signal mean value

$$\tilde{y}(t) = A_m \sin(\omega_m t). \tag{3b}$$

Equations (3a) and (3b) will produce an analytic signal of the form

$$Y(t) = y(t) + j\tilde{y}(t) = A(t) \exp(j\omega t), \tag{4}$$

where $A^2(t) = 2A_m M \cos(\omega_m t) + M^2 + A_m^2$ is the nonsymmetric signal envelope squared, and $\omega(t) = \omega_m \dfrac{A_m M \cos(\omega_m t) + A_m^2}{A^2(t)}$ is the nonsymmetric signal instantaneous frequency. From equation (4), it can be seen that the signal envelope consists of two different parts. There is a slow-varying part, which includes a sum of the amplitude squared together with the mean value squared, and also a fast-varying (oscillating) part, which is the product of the amplitude and the mean value with the function $\cos(\omega_m t)$. For such a case, it is possible to separate the slow and the fast (oscillating) parts of a signal envelope (mentioned above) by using an ordinary filtration in the frequency domain. Thus, only the fast part, $A_f^2(t)$, will be retained after high-pass filtration of the square of the signal envelope: $A_f^2(t) = 2A_m M \cos(\omega_m t)$. This new function is now just a monocomponent signal. Repeating the application of the HT, the new envelope extraction is readily achieved: $|A_f^2| = 2A_m M$. Then, after an algebraic operation, we will get a simple formula for each nonsymmetric amplitude estimation: $A_{1,2} = \sqrt{A^2 - A_f^2 \pm |A_f^2|}$, where A_1 is the positive amplitude, A_2 is the negative amplitude, A is the envelope of the nonsymmetric signal, A_f is the fast oscillating part of a signal envelope, and $|A_f^2|$ is the envelope (result) of the repeated application of the HT.

Let us consider the next approximation of a nonsymmetric signal $y(t)$ as a combination of two harmonics with different frequencies ω_1, ω_2 and the same amplitude A_m. The difference between the positive and the negative harmonic will eventually produce a nonzero mean value of the signal M_ω:

$$y(t) = \begin{cases} A_m \cos\omega_1 t + M_\omega, & \text{if } y > 0 \\ A_m \cos\omega_2 t + M_\omega, & \text{if } y \le 0 \end{cases}, \tag{5}$$

where $M_\omega = \frac{2A_m}{\pi}\frac{\omega_2 - \omega_1}{\omega_2 + \omega_1}$ is the mean value of the nonsymmetric signal. The instantaneous frequency of the signal will now be biased due to the nonzero mean value equation (4):

$$\omega(t) = \begin{cases} \omega_1 b, & \text{if } y > 0 \\ \omega_2 b, & \text{if } y \le 0 \end{cases}, \tag{6}$$

where $b = (A_m M_\omega \cos\omega_m t + A_m^2)/(A^2(t))$. To simplify the last equation, we assume that the mean value M_ω of a nonsymmetric signal is always less than the amplitude of the signal, $M_\omega < A_m$:

$$\omega(t) = \omega_{1,2}\left(1 + \frac{M_\omega}{A_m}\cos\omega_m t\right) \bigg/ \left(1 + 2\frac{M_\omega}{A_m}\cos\omega_m t\right), \tag{7}$$

where $\omega_{1,2} = \omega_1$ if $y > 0$; $\omega_{1,2} = \omega_2$ if $y < 0$. The obtained equation (7) explains that the instantaneous frequency of the nonsymmetric cycle, associated with the lesser frequency, is slightly less than the initial frequency. Correspondingly, the instantaneous frequency associated with the larger frequency is moderately larger than the initial frequency. After using a separate low-pass filtration of the instantaneous frequency associated with the positive and the negative portions of the signal, we will get two biased frequencies of the nonsymmetric signal (equation (5)): $\langle\omega_{\text{pos,neg}}\rangle = \omega_{1,2}\left((1 \pm M_\omega^2)/(A_m^2)\right)$. The obtained bias value is very small. For example, in extreme cases, when $\omega_2 = 2\omega_1$, the bias is only 10%, suggesting that the bias value could be neglected. In consequence, the resultant formula for the component frequencies takes the form $\omega_{1,2} = \langle\omega_{\text{pos,neg}}\rangle$. The use of the developed technique could result in a more precise estimation of both the amplitude and the frequency of nonsymmetric vibration signals.

2.3. The Hilbert Transform Identification Technique

A vibration signal suitable for the HT identification should be a monocomponent signal derived from a single-degree-of-freedom system directly or obtained from a multi-degree-of-freedom system after special decomposition or after band-pass filtration. This initial signal $y(t) = A(t)\cos\psi(t)$—where $y(t)$ is the vibration signal (real valued function), $A(t)$ is the envelope (instantaneous amplitude), and $\psi(t)$ is the instantaneous phase—is assumed to be a free solution of a nonlinear vibration system with frequency dependent damping $\ddot{y} + 2h(\dot{y})\dot{y} + k(y)y = 0$, where $2h(\dot{y})\dot{y}$ is the nonlinear viscous damping force characteristic and $k(y)y$ is the nonlinear elastic force characteristic. It is desirable to recover nonlinear

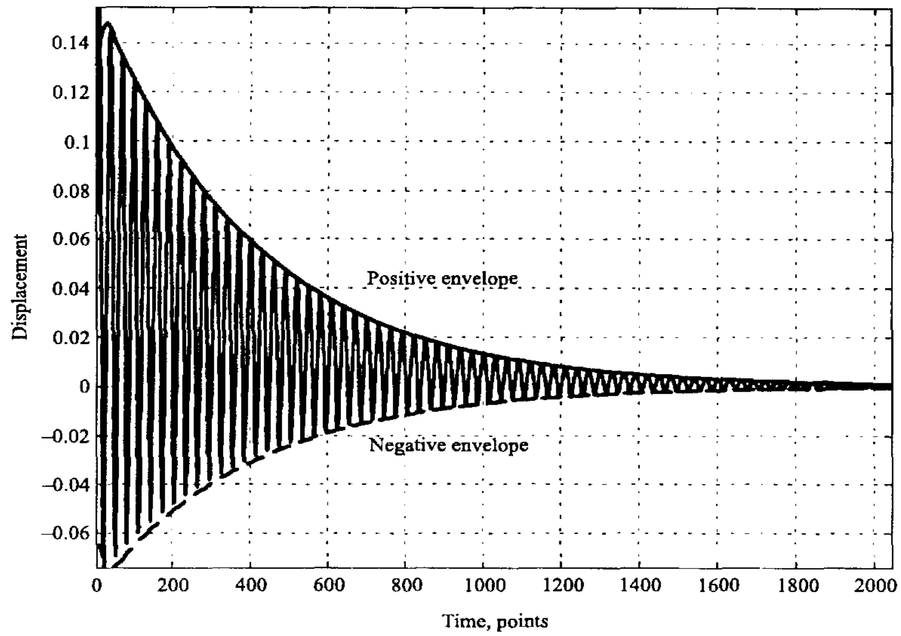

Figure 2. Bilinear nonsymmetric system free vibration.

backbones and damping curves from the measured vibration signal. For this purpose, some resultant equations could be used (Feldman, 1994a):

$$\begin{aligned} \omega_0^2 &= \dot{\psi}^2 - \frac{\ddot{A}}{A} + \frac{2\dot{A}^2}{A^2} + \frac{\dot{A}\ddot{\psi}}{A\dot{\psi}} \\ h(t) &= -\frac{\dot{A}}{A} + \frac{\ddot{\psi}}{2\dot{\psi}}, \end{aligned} \tag{8}$$

where $\omega_0(t)$ is the instantaneous undamped natural frequency of the system; $h(t)$ is the instantaneous damping coefficient of the system, $\dot{\psi}$, and A are the instantaneous frequency and envelope (amplitude) of the vibration with their first and second derivatives. Algebraically, equation (8) means that the HT identification method uses the initial displacement, velocity, and acceleration together.

3. APPLICATION OF THE HILBERT TRANSFORM TO NONLINEAR SYSTEMS SIMULATION

All simulation examples demonstrate the performance that can be achieved using the proposed technique. To focus our nonsymmetric signal processing on the effects of the nonlinear vibration systems identification, we also use the HT identification method (Feldman, 1994a).

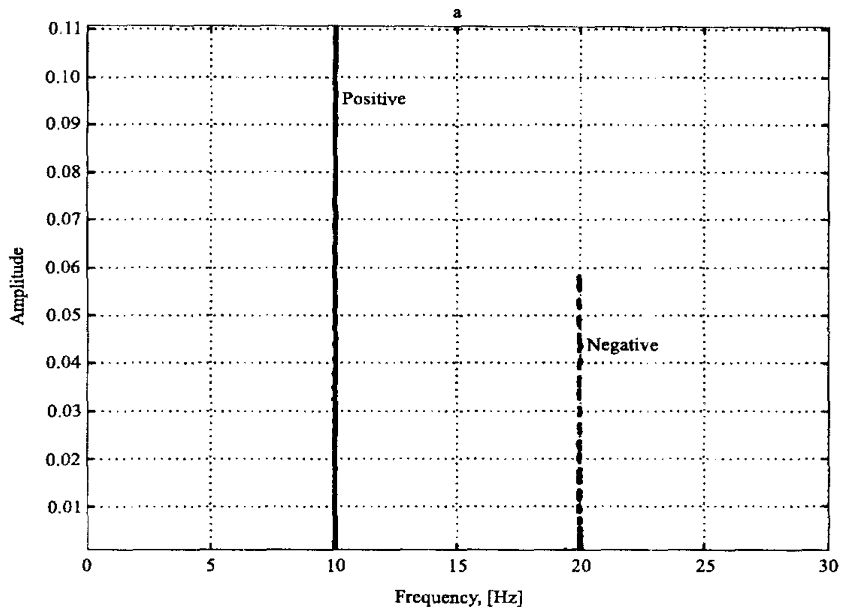

Figure 3(a). Estimated force characteristic of a bilinear system: backbone.

3.1. Nonsymmetric Bilinear Free Vibration

Consider the initial simulated signal of the free vibration of a nonsymmetric bilinear system:

$$\ddot{y} + 2\dot{y} + F(y) = 0$$

$$F(y) = \begin{cases} (20\pi)^2 y, & \text{if } y > 0 \\ (40\pi)^2 y, & \text{if } y \leq 0 \end{cases}, \tag{9}$$

which is shown in Figure 2 together with the separated envelopes. By applying the HT identification technique to the signal, backbones and damping curves shown in Figure 3 are obtained. In the case shown, it is obvious that the natural frequencies are constant (correspondingly 10 and 20 Hz), and the damping coefficient also is a constant ($h = 1, s^{-1}$).

3.2. Free Vibration of a Nonsymmetric System With Two Cubic Stiffnesses

The next example is the case of nonsymmetric free vibration with two cubic stiffnesses:

$$\ddot{y} + 2\dot{y} + F(y) = 0$$

$$F(y) = \begin{cases} (20\pi)^2 (1 + 5y^2) y, & \text{if } y > 0 \\ (40\pi)^2 (1 - 3y^2) y, & \text{if } y \leq 0 \end{cases}. \tag{10}$$

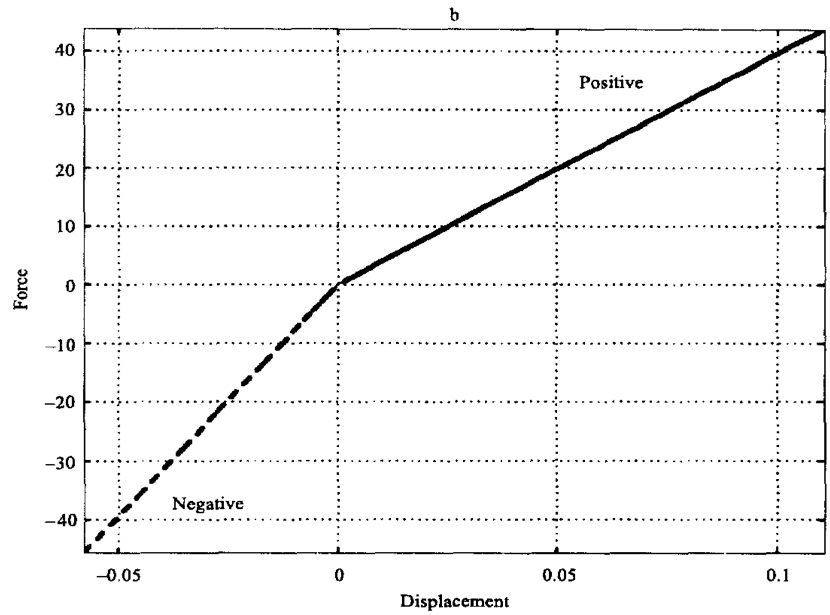

Figure 3(b). Estimated force characteristic of a bilinear system: spring force characteristic.

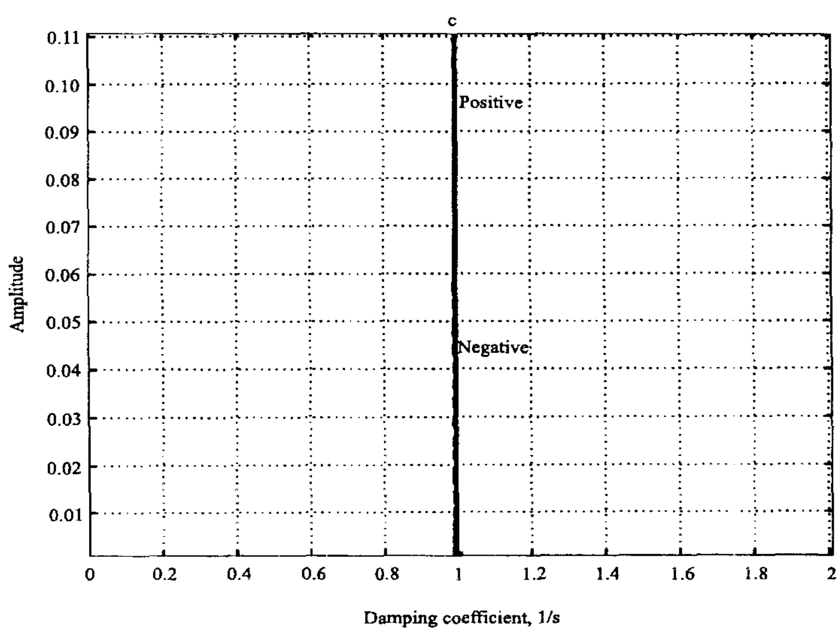

Figure 3(c). Estimated force characteristic of a bilinear system: damping curvec.

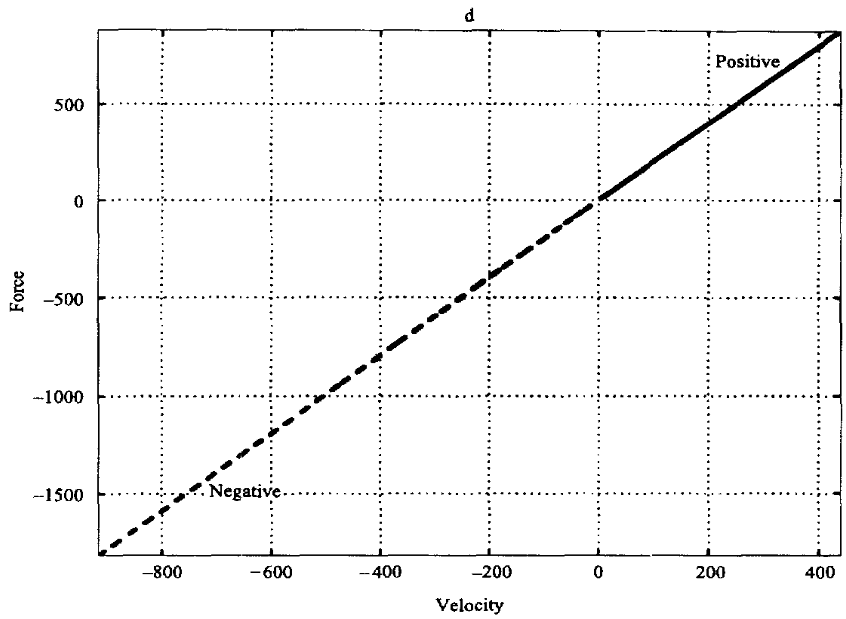

Figure 3(d). Estimated force characteristic of a bilinear system: friction force characteristic.

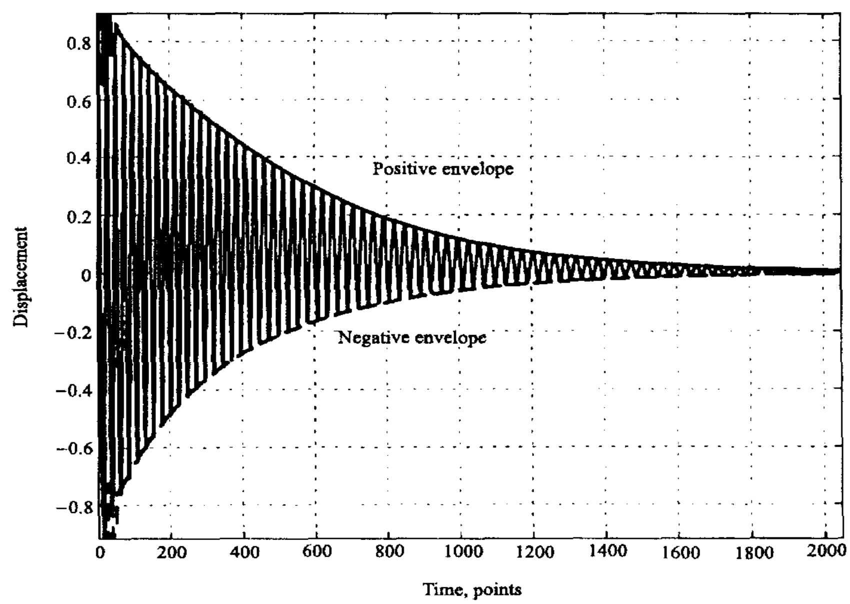

Figure 4. Nonsymmetric free vibration of two cubic stiffnesses.

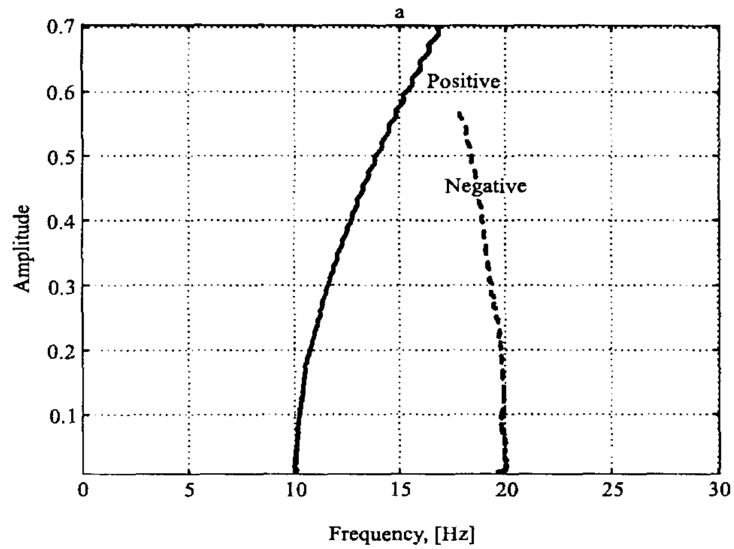

Figure 5(a). Estimated force characteristic of two cubic stiffnesses: backbone.

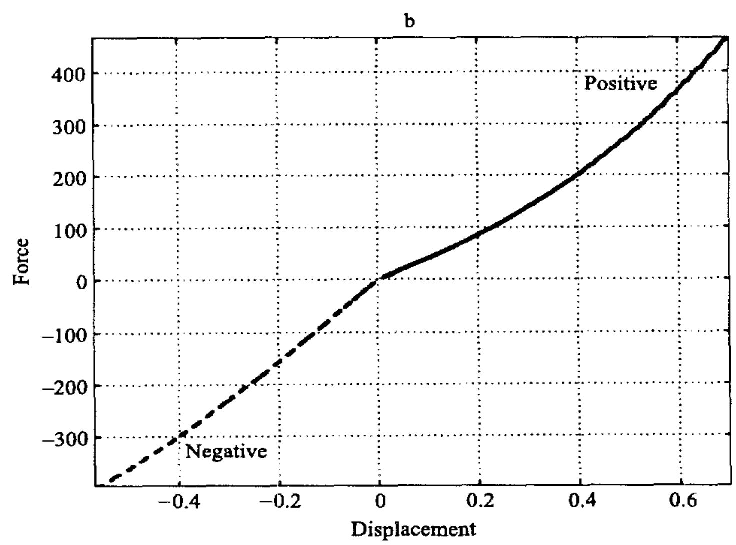

Figure 5(b). Estimated force characteristic of two cubic stiffnesses: spring force characteristic.

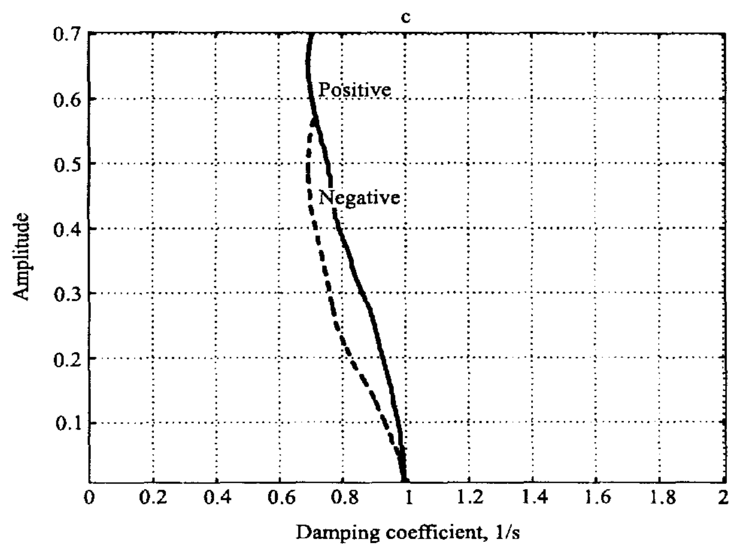

Figure 5(c). Estimated force characteristic of two cubic stiffnesses: damping curve.

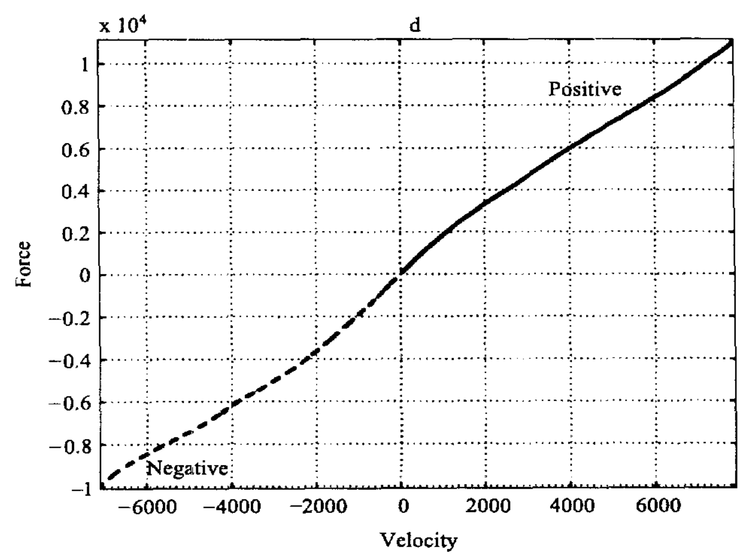

Figure 5(d). Estimated force characteristic of two cubic stiffnesses: friction force characteristic.

Computer simulation, performed for 1,024 points with a sample frequency 1 Hz, is shown in Figure 4. The two obtained backbones shown in Figure 5 indicate the varying value of the frequency of the system. The hardening backbone for the positive displacement and the softening backbone for the negative displacement agree with the initial nonsymmetric Duffing equation (10).

4. THEORETICAL BACKGROUND: DYNAMIC BEHAVIOR OF A ROTOR WITH A CRACKED SHAFT

4.1. Diagnosis of Cracks in Rotating Shafts

Investigations concerning the dynamic behavior of a rotor with a cracked shaft receive increasing interest, especially those aiming at the diagnosis of the damage. The reason is quite obvious: severe damages in power plants have been reported in the past, many of them due to fatigue cracks in the turbine shaft (Haas, 1977; Höxtermann, 1988; Muszynska, 1992). As a consequence, tools for monitoring and diagnosis are being developed to avoid such catastrophic failures. The aim is to diagnose cracks at an early level, so that a sound calculation of the remaining lifetime can be performed.

The paper by Wauer (1990) summarizes the efforts performed in the field of the modeling and detection of cracks. The first investigations performed were restricted to the basic phenomena occurring due to a cracked rotor shaft. They were based on the assumption of a simple Jeffcott-rotor model, which consists of an elastic massless shaft on hinged supports, with a rigid disk placed in the middle of the shaft. The location of the crack is supposed to be next to the disk (Gasch, 1976). The governing phenomenon for the dynamic behavior of a cracked rotor is the breathing of the crack (i.e., the opening and closing of the crack during the rotation of the shaft). Generally, the breathing depends on the vibrations of the rotor and therefore on the momentary displacements. Therefore, the system behavior is described by nonlinear differential equations.

4.2. A Finite Beam Element With a Crack: The Theis Model

In real life, the dynamic behavior of turbomachinery is governed by weight dominance: The vibration amplitudes of the rotor are small compared to its static displacement. Then, simplified linear differential equations of motion can be derived (see, e.g., Dimarogonas and Papadopoulos, 1983; Mayes and Davies, 1983). The crack can be assumed as an external load (crack load), and the breathing is described as a function of the angle of rotation φ.

Theis (1990) has developed a finite beam element with a breathing crack that takes into account all six degrees of freedom of the Bernoulli beam theory and is based on the work of Papadopoulos and Dimarogonas (1988). The additional compliance due to the crack is derived based on fracture mechanical considerations via the energy release rate. Contrary to earlier works, the Theis model considers the semi-open crack in addition to the open and the closed crack. The transition between these states is described by heuristic rating functions, and the breathing of the crack depends on the vector of bending moments in the cracked cross section. This crack model requires bending dominance, which means that the breathing only results from the bending vibrations, which in turn influence the lateral and torsional

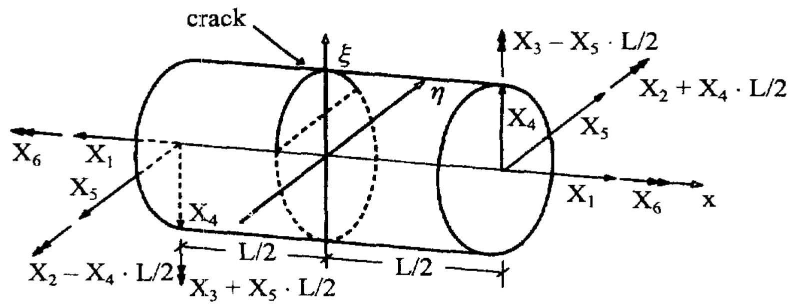

Figure 6. Crack model of Theis.

vibrations via cross-coupling terms. No additional demands concerning the torsional degrees of freedom are required; however, lateral forces cannot be taken into account. Therefore, the crack model is not valid for critical frequency ranges concerning the lateral vibrations.

The Theis model allows consideration of the coupling between the bending vibrations and the lateral and torsional vibrations due to the crack. In the following, however, the governing equations are given for bending vibrations only. Furthermore, weight dominance is assumed. Employing the small-amplitude approximation, the following linear differential equations can be derived in which the additional dynamics due to the crack are modeled as external crack loads acting on the system (Theis, 1990; Seibold and Weinert, 1996):

$$\underline{M}\Delta\ddot{\underline{q}}(\varphi) + \underline{D}\Delta\dot{\underline{q}}(\varphi) + \underline{K}_0\Delta\underline{q}(\varphi) = \underline{F}_R(\varphi) + \underline{F}_U(\varphi), \tag{11}$$

with $\underline{M}$ and $\underline{D}$ being the mass and damping matrices and $\underline{F}_U$ being the unbalance excitation. The crack loads are denoted as

$$\underline{F}_R = -\Delta\underline{K}(\varphi)\,\underline{q}_s\,. \tag{12}$$

Theis (1990) described how the additional compliance due to the crack can be derived via the energy release rate based on fracture mechanical considerations. To facilitate the application to model-based damage diagnosis, the crack loads can be approximated by the following polynomial functions (Seibold, 1995):

$$\underline{F}_R(a,\varphi) = \left(\sum_{i=0}^{n} a^i \underline{P}_i\right)\underline{\gamma}(\varphi) = \underline{R}(a)\,\underline{\gamma}(\varphi), \tag{13}$$

where a is the depth of the crack, $\underline{P}_i$ are constant matrices of coefficients independent of a and φ, and

$$\underline{\gamma}(\varphi)^T = [1\ \sin\varphi\ \sin 2\varphi\ \ldots\ \sin k\varphi\ \cos\varphi\ \cos 2\varphi\ \ldots \cos k\varphi] \tag{14}$$

is a function of the angle of rotation φ.

The Theis model does not require weight dominance, and it can be modified for nonconstant speeds of rotation. Still, one quite severe restriction needs to be mentioned:

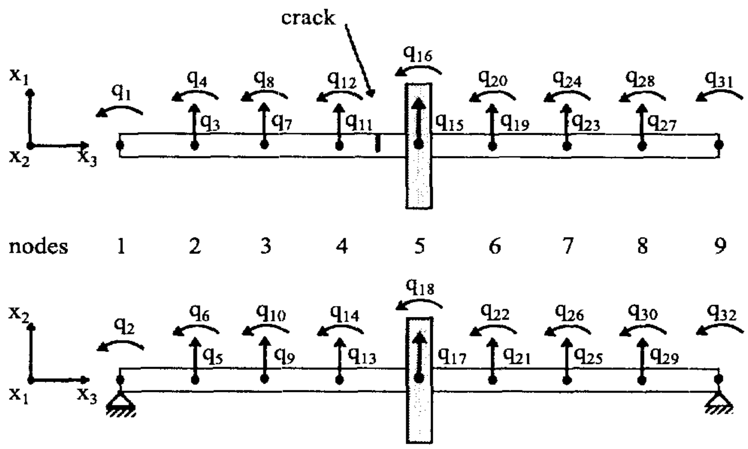

Figure 7. Finite element model of a rotor with a cracked shaft.

The model is only valid for cracks with a depth less than the radius of the shaft. However, the modified Theis model, according to equations (13) and (14), facilitates the application to damage diagnosis. Based on the concept of modeling the crack as external loads, the crack element can be easily implemented in existing finite element (FE) programs. Figure 6 shows the crack model: The crack, which need not be located in the middle of the beam element, is mapped as external forces and moments X_i. This crack element then can be added to an FE model of a rotor (see Figure 7).

5. MULTIHYPOTHESIS TESTING WITH A BANK OF KALMAN FILTERS

Multihypothesis testing based on a bank of Kalman filters is a powerful tool for detecting the location of damage. The theoretical background and an application to cracks in rotating shafts are described in Seibold and Weinert (1996). This model-based approach requires a suitable model of the system—for instance, the FE model shown in Figure 7. The idea is to design different Kalman filters for different damage hypotheses (bank of filters, Figure 8). In our case, supposing we want to detect the location of a crack in a rotor modeled according to Figure 7, nine different hypotheses are needed: the zero hypothesis based on an FE model of the rotor without a crack and eight hypotheses based on FE models of the rotor with a crack in beam elements 1 through 8. The differences between model prediction $\hat{\underline{z}}_{k+1/k}$ and measurements $\underline{y}_{k+1}$ are called innovations $\underline{\nu}$. Each Kalman filter generates these innovations for every time step k:

$$\underline{\nu}_{k+1} = \underline{y}_{k+1} - \underline{C}\hat{\underline{z}}_{k+1/k}\,, \tag{15}$$

where $\underline{y}_{k+1}$ is the vector of measurements at time step $k+1$, $\hat{\underline{z}}_{k+1/k}$ is the model prediction for the time step $k+1$, and $\underline{C}$ is the measurement matrix. The measurements $\underline{y}_{k+1}$ are noisy, and this measurement noise is usually normally distributed, uncorrelated, and white. Now, if the model is correct (i.e., in our case, if the crack is assumed at the correct location), then the

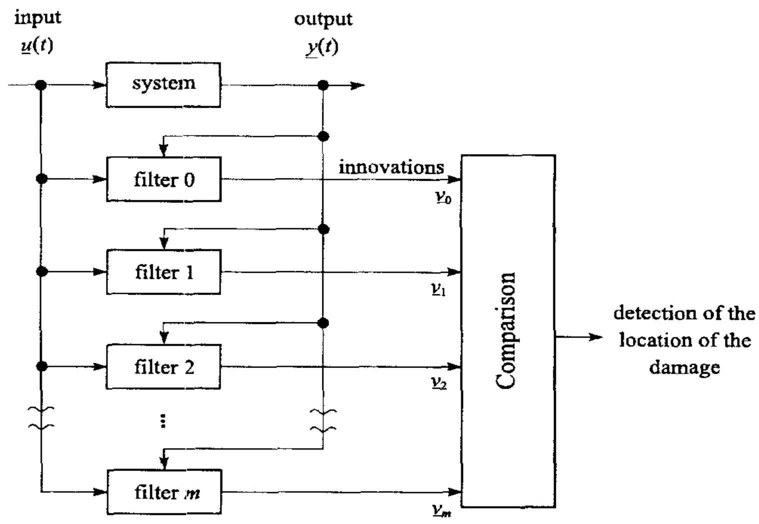

Figure 8. Bank of filters.

difference between model prediction $\hat{z}_{k+1/k}$ and measurements y_{k+1} is just the measurement noise. Therefore, by statistically analyzing the innovations of each Kalman filter in the bank of filters, the location of the crack can be determined because the filter with the correct hypothesis will yield the smallest innovations with the above-mentioned statistical properties. Furthermore, if extended Kalman filters (EKF) are employed, a parallel state and parameter estimation can be performed, and the depth of the crack can be calculated too.

6. ROTOR TEST RIG: IDENTIFICATION OF A CRACK IN THE ROTOR SHAFT

A simple rotor test rig was built to apply the proposed procedure to real measurements (see Figure 9). The test rig consists of a shaft with radius $R = 9$ mm on hinged supports. A disk is mounted in the middle. Initiated by a notch of about 2 mm depth, a transverse crack in the shaft at a location close to the disk is introduced. Two kinds of vibrations are measured: free vibrations of the disk initiated by an impulse and stationary vibrations at constant speed. Then, static overloads are applied using a special apparatus. This results in dark lines (benchmarks) on the crack face. After the experiment, the measurements taken can be related to the benchmarks and to the actual crack depths. In this way, the results of the identification can be checked. The experimental setup is described in detail in Seibold (1995).

6.1. Detection of the Crack With the HT Approach

An experimental identification of the rotor structure with a notch and crack was made on the basis of four separate measurements (512 time steps) of free vibrations of the disk (crack at the lowest position). In this experiment, the depth of the crack was 5 mm. Free vibrations were

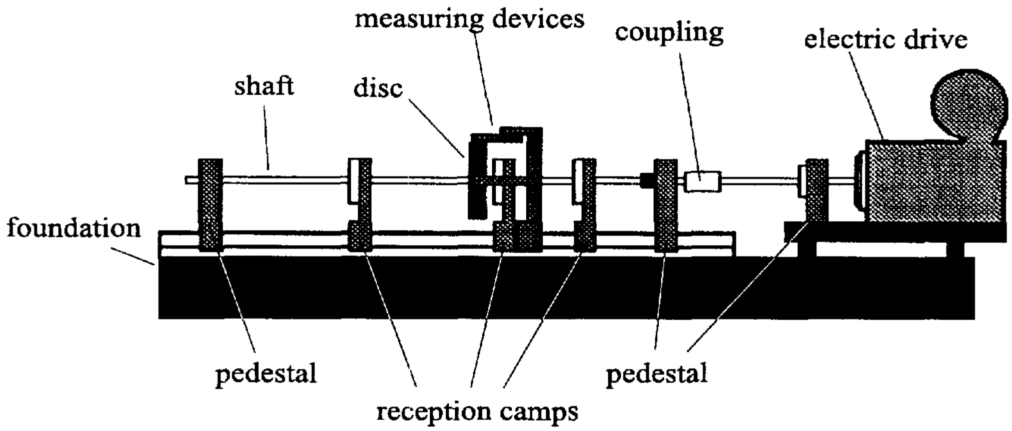

Figure 9. Rotor test rig.

picked up from the nonrotating rotor after exciting the system with an impulse hammer. The proposed HT method enables us to separate the measured nonsymmetric vibration into two different parts. The first part (Figure 10, bold line) describes system behavior for only positive displacement and the second part (Figure 10, dashed line) for only negative displacement. The obtained results of the HT identification, shown in Figure 10, indicate the closely spaced positive and the corresponding negative backbones of the four separate measurements. The tested system has a strong nonsymmetric elastic force characteristic: The positive movement exhibits smaller values of the natural frequency (25.5-26 Hz). The difference between the natural frequencies for the positive and the negative movement is about 2 Hz.

The system also has a small nonlinear elastic force characteristic, dissimilar for the positive and the negative movement. The positive movement backbone looks like a hardening nonlinear spring. On the contrary, the negative movement backbone shows small softening nonlinear spring characteristics. The tested system has a symmetric friction characteristic. The estimated friction force characteristics possess a strong, dry friction nature.

6.2. Detection of the Location of the Crack With the Multihypothesis Approach

The results of the previous section clearly indicate the presence of a crack. Now, the location and depth of this crack can be determined employing the multihypothesis approach described in Section 5 and the measured vibrations of the disk at constant speed. Considering our model of the rotor (Figure 7), nine damage hypotheses and therefore a bank of nine EKFs is needed. One filter is based on the null hypothesis "no crack," and eight filters have to be designed based on the hypothesis "crack in beam element number i." These eight filters are based on an FE model of the rotor with a crack in the specific beam element and perform a parallel state and parameter estimation in which the parameter to be estimated is the depth of the crack. To avoid excessive computation time, a modal condensation to the first four bending eigenforms is performed.

Figure 11 shows the identification of the crack depth a based on the true hypothesis number 4. The true crack depth is 5 mm, and the identified value is 5.2 mm. The parameter

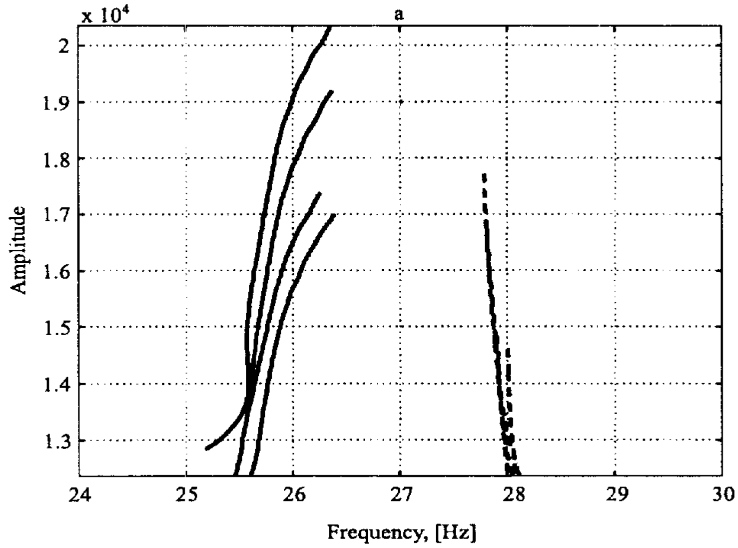

Figure 10(a). Estimated force characteristic of a crack and notch structure: backbone.

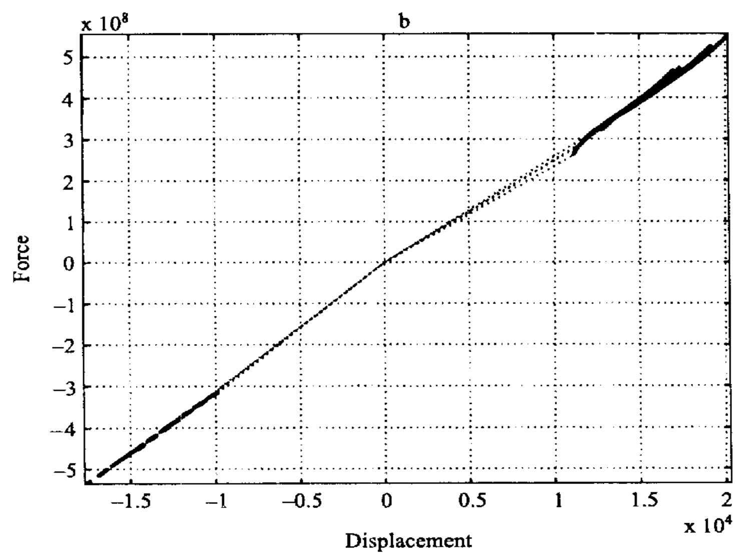

Figure 10(b). Estimated force characteristic of a crack and notch structure: spring force characteristic.

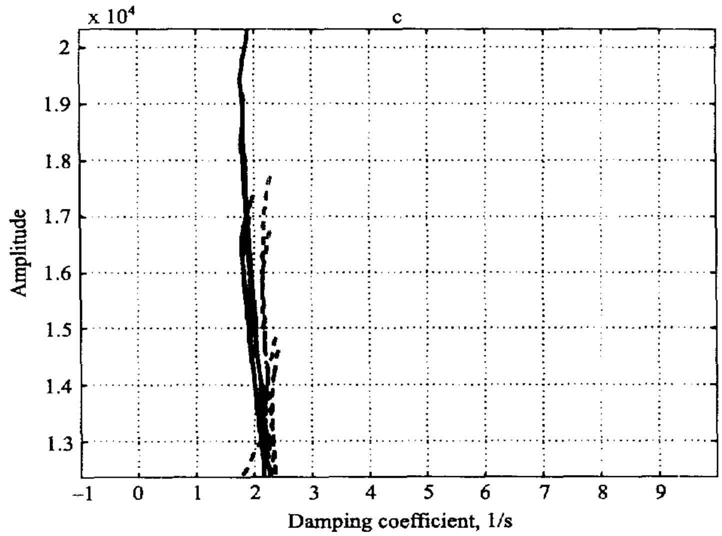

Figure 10(c). Estimated force characteristic of a crack and notch structure: damping curve.

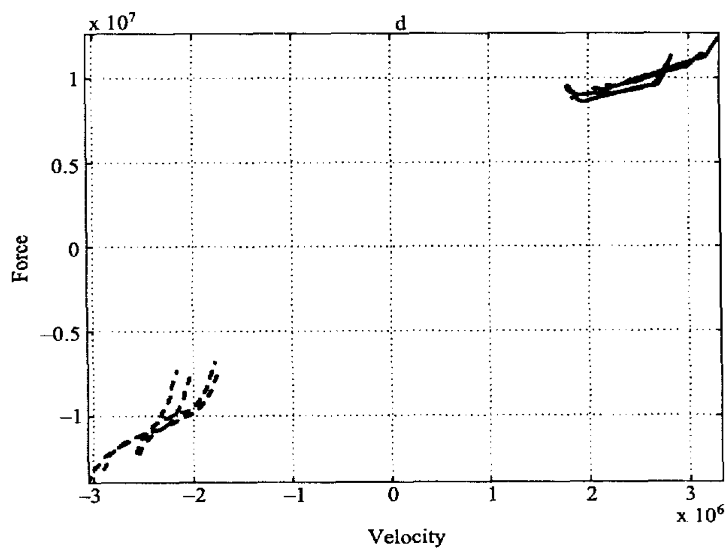

Figure 10(d). Estimated force characteristic of a crack and notch structure: friction force characteristic.

converges quickly. Figure 12 shows the mean of the related standard deviations of the different damage hypotheses. If the detection of the location is successful, the correct hypothesis should possess the smallest standard deviation (Mehra and Peschon, 1971).

As stated above, the measurement setup only allows a measurement of the displacements of the disk. It is not possible to pick up measurements next to the pedestals due to the diameter of the shaft, which is relatively small. Therefore, it is impossible to determine whether the crack is on the left-hand or right-hand side of the disk, and symmetric hypotheses such as 1 and 8, 2 and 7, 3 and 6, and 4 and 5 possess the same standard deviations. Still, it is obvious from Figure 12 that the crack is in one of the beam elements next to the disk (i.e., beam element number 4 or 5).

The computations were performed using PC-Matlab. For the processing of 2,000 time steps, each filter in the bank needs less than 30 seconds of computation time.

In Seibold and Weinert (1996), it is shown that the crack location can be determined very well if more sensors are available. Of course, a bank of Kalman filters may also be designed on the basis of a nonlinear model of the cracked rotor. In Seibold (1995, 1997), it was shown that the crack depth can be identified based on a nonlinear Jeffcott-rotor model. Furthermore, smaller cracks can be diagnosed very well. It is also possible to consider nonconstant speeds of rotation.

7. COMPARISON TO OTHER DIAGNOSTIC PROCEDURES AND CONCLUSION

Recently, the problem of damage detection and diagnosis has been tackled by many researchers from different fields. Most of the approaches are based on the investigation of modal quantities, such as changes in eigenfrequencies and eigenforms. A recent paper showed that the size and location of a crack in a rotor can be calculated by investigating the changes in the first four harmonics (Hachmann and Popp, 1997). The approach is very interesting and validated by measurements taken at a rotor test rig. However, the authors state that the eigenfrequencies have to be determined very accurately, which is in practice not always possible. Furthermore, small cracks have only insignificant influences on the eigenfrequencies, so that they cannot be detected by monitoring the eigenfrequencies alone.

A completely different approach is suggested by Fritzen, Jennewein, and Buchen (1996). They propose the employment of a model representing the undamaged vibrating structure and a local description of the damage and show that multiple cracks in a steel frame, as well as a "lost mass" in a spatial structure, can be identified quite accurately. Up to now, only nonrotating structures have been treated.

Damage detection was the main subject of the last International Modal Analysis Conference in February 1997. The paper by Worden (1997) describes how artificial neural networks can be employed for condition monitoring and applies the method to a simulated 3-degree-of-freedom system. Recently, the research in this area often has been associated with methods of novelty or anomaly detection, very similar to the idea of multihypotheses testing. This can also be stated about the approach presented by Abdelghani, Basseville, and Beneviste (1997). In their study, damage is diagnosed by a comparison to a reference model. For each hypothesized damage, test statistics are generated, and the statistics measure the likelihood of the most likely change (i.e., damage) in the structure.

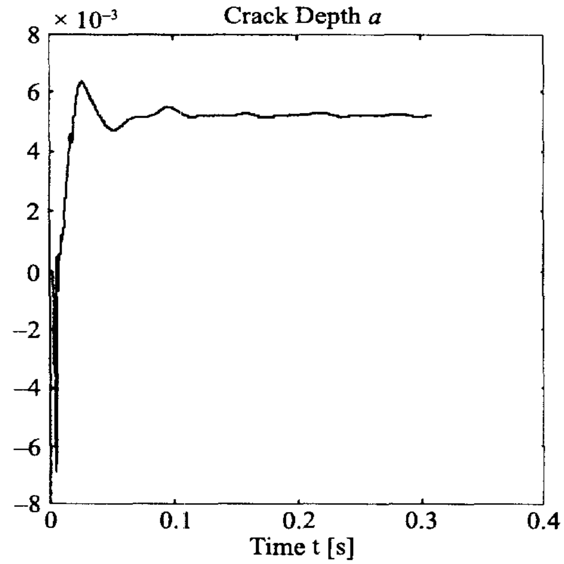

Figure 11. Identification of the crack depth a; hypothesis number 4.

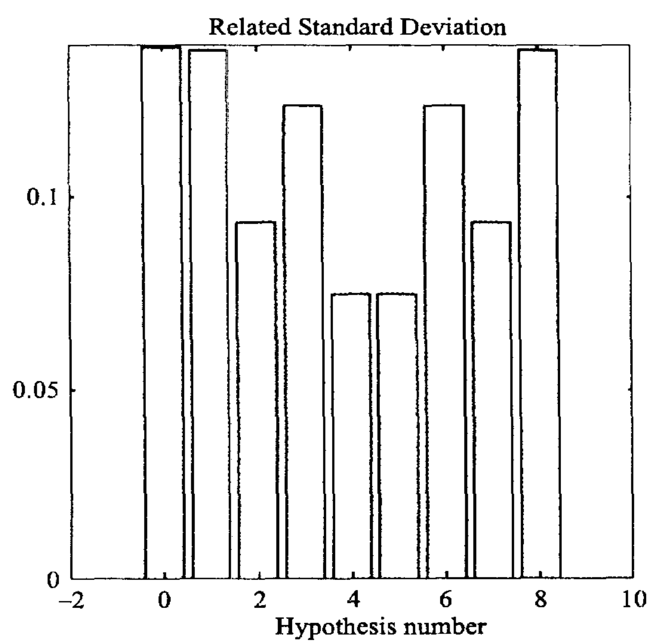

Figure 12. Related standard deviations (mean) of the different hypotheses.

According to the knowledge of the authors, there is no combined approach documented in the literature similar to the one presented in this paper, except for a paper published by one of the authors (Bucher and Seibold, 1997). The modal procedures mentioned above, as well as the purely signal-based procedures in general, yield excellent results concerning the detection of damage, but usually their drawback is the inherent difficulty to determine the location and extent of damage. This gap can be overcome very well by a model-based approach, which, on the other hand, is quite time-consuming and usually not applicable for on-line monitoring. Furthermore, with model-based procedures, it might be difficult to distinguish between specific damages, such as a crack and an increasing unbalance. Therefore, a combination of the two methodologies will yield an improved detectability of damages at early stages compared to using each approach separately. However, it is not possible to quantify this improved detectability. Generally, the success of a signal-based approach depends very much on the initial physical knowledge of the user. It may yield valuable information about the type of the damage, but the extent can only very rarely be calculated: The results are of a qualitative nature. However, the knowledge about the type of the damage obtained by the signal-based approach is a very valuable basis for an improved model-based diagnosis, which will yield a quantitative estimate of the size and location of the damage. A purely model-based approach, on the other hand, can fail if no initial knowledge about the damage is available. The reason is that a multitude of different types of damages would have to be considered, and it would be a difficult (and time-consuming) task to distinguish damages with similar effects on the measurements (e.g., an increasing unbalance and a crack in the rotor shaft). True progress in the area of diagnostics can be made if signal- and model-based diagnoses are combined.

In this paper, the applicability to the diagnosis of cracks in rotors was proven. In the first simulated example, the application of the HT for the decomposition of nonsymmetric signals was shown. Then, the combined methodology was applied to a rotor test rig with a cracked shaft. The results of the HT clearly indicated the type of damage, a crack in the rotor shaft, so that subsequently a bank of Kalman filters based on a suitable model of the damage could be designed. By multihypothesis testing, the location and the depth of the crack could be determined.

Further research will be devoted to investigating the applicability to smaller cracks, as well as to other types of damages.

Acknowledgment. The project is partly financed by the German Research Association (DFG) under contract no. Se 578/5-1, which is highly appreciated. The authors also appreciate the valuable remarks of the reviewers, which helped to improve the quality of the paper.

REFERENCES

Abdelghani, M., Basseville, M., and Beneviste, A., 1997, "In-operation damage monitoring and diagnostics of vibrating structures, with application to off-shore structures and rotating machinery," in Proceedings of the *15th IMAC, International Modal Analysis Conference, Vol. II*, Orlando, FL, 1815-1830.

Bucher, I. and Seibold, S., 1997, "Using combined temporal and spatial information in multi-hypothesis based damage detection for rotating machines," in Proceedings of the *15th IMAC, International Modal Analysis Conference, Vol. I*, Orlando, FL, 870-876.

Dimarogonas, A. D. and Papadopoulos, C. A., 1983, "Vibration of cracked shafts in bending," *Journal of Sound and Vibration* **91**(4), 583-593.

Feldman, M., 1985, "Investigation of the natural vibrations of machine elements using the Hilbert transform," *Soviet Machine Science* **2**, 44-47.

Feldman, M., 1994a, "Non-linear system vibration analysis using Hilbert transform: I. Free vibration analysis method FREEVIB," *Mechanical Systems and Signal Processing* **8**(2), 119-127.

Feldman, M., 1994b, "Non-linear system vibration analysis using Hilbert transform: II. Forced vibration analysis method FORCEVIB," *Mechanical Systems and Signal Processing* **8**(3), 309-318.

Feldman, M., 1997, "Vibration analysis of non-symmetric elastic force systems via the Hilbert transform," in Proceedings of the *15th IMAC, International Modal Analysis Conference, Vol. I*, Orlando, FL, 1017-1022.

Fritzen, C.-P., Jennewein, D., and Buchen, D., 1996, "Model based damage detection from vibration data," in Proceedings of *ISMA 21, International Conference on Noise and Vibration Engineering*, Lourain, Belgium, 1017-1031.

Gasch, R., 1976, "Dynamic behavior of a simple rotor with a cross-sectional crack," *Conference on Vibrations in Rotating Machinery, IMechE Conference Publications*, University of Cambridge, UK.

Haas, H., 1977, "Großschäden durch Turbinen- oder Generatorläufer, entstanden im Bereich bis zur Schleuderdrehzahl," *Der Maschinenschaden* **50**(6), 195-204 (in German).

Hachmann, I. and Popp, K., 1997, "Ermittlung des Rißortes angerissener Wellen im ruhenden und rotierenden System," *SIRM'97 Schwingungen in Rotierenden Maschinen IV*, H. Irretier, R. Nordmann, and H. Springer, eds., Vieweg Verlag, Braunschweig/Wiesbaden, 191-198.

Höxtermann, E., 1988, "Erfahrungen mit Schäden in Form von Anrissen und Brüchen an Dampfturbinenwellen, Radscheiben und Generatorläufern," *VGB Technisch-Wissenschaftliche Berichte Wärmekraftwerke—VGB-TW 107*, Berlin (in German).

Mayes, I. W. and Davies, W.G.R., 1983, "Analysis of the response of a multi-rotor-bearing system containing a transverse crack in a rotor," *ASME Design Engineering Technical Conference*, Dearborn, MI, Paper 83-DET-84.

Mehra, R. K. and Peschon, J., 1971, "An innovations approach to fault detection in dynamic systems," *Automatica* **7**, 637-640.

Mitra, S. K. and Kaiser, J. F., 1993, *Handbook for Digital Signal Processing*, Wiley-Interscience, New York.

Muszynska, A., 1992, "Vibrational diagnostics of rotating machinery malfunctions," in *Course on Rotor Dynamics and Vibration in Turbomachinery*, von Karman Institute for Fluid Dynamics, Belgium.

Papadopoulos, C. A. and Dimarogonas, A. D., 1988, "Coupled longitudinal and bending vibrations of a cracked shaft," *Journal of Vibration, Acoustics, Stress and Reliability in Design* **110**, 1-8.

Seibold, S., 1995, *Ein Beitrag zur modellgestützten Schadendiagnose bei rotierenden Maschinen*, VDI-Fortschrittberichte, VDI-Verlag, 11/219, Düsseldorf (in German).

Seibold, S., 1997, "Identification of physical parameters employing an instrumental variables technique," *Journal of Mechanical Systems and Signal Processing* **11**(3), 425-439.

Seibold, S. and Weinert, K., 1996, "A time domain method for the localization of cracks in rotors," *Journal of Sound and Vibration* **195**(1), 57-73.

Theis, W., 1990, *Längs- und Torsionsschwingungen bei quer angerissenen Rotoren: Untersuchungen auf der Grundlage eines Rißmodells mit 6 Balkenfreiheitsgraden*, VDI-Verlag, Düsseldorf, Reihe 11, Nr. 131 (in German).

Wauer, J., 1990, "On the dynamics of cracked rotors: A literature survey," *Applied Mechanics Review* **43**, 13-17.

Williams, J. H. and Davies, A., 1992, "System condition monitoring: An overview," *Noise and Vibration Worldwide* **23**(9), 25-29.

Worden, K., 1997, "Damage detection using a novelty measure," in Proceedings of the *15th IMAC, International Modal Analysis Conference, Vol. I*, Orlando, FL, 631-637.